Hierarchical model predictive control for energy management of power-to-X systems

Kaya, Oguzhan; Van Der Roest, Els; Vries, Dirk; Keviczky, Tamas

DOI
10.1109/ISGT-Europe47291.2020.9248892

Publication date
2020

Document Version
Final published version

Published in
Proceedings of the IEEE PES Innovative Smart Grid Technologies Europe, ISGT-Europe 2020

Citation (APA)
Kaya, O., Van Der Roest, E., Vries, D., & Keviczky, T. (2020). Hierarchical model predictive control for energy management of power-to-X systems. In *Proceedings of the IEEE PES Innovative Smart Grid Technologies Europe, ISGT-Europe 2020* (pp. 1094-1098). IEEE. https://doi.org/10.1109/ISGT-Europe47291.2020.9248892

2020 IEEE PES Innovative Smart Grid Technologies Europe (ISGT-Europe)
Virtual, October 26-28, 2020

Hierarchical Model Predictive Control for Energy Management of Power-to-X Systems

Oguzhan Kaya, Els van der Roest, Dirk Vries, Tamas Keviczky

Abstract—**This paper presents the application of Hierarchical Model Predictive Control (HMPC) as an energy management framework for a multi-timescale mixed-energy system, i.e., Power-to-X (PtX). The goal of the energy managing controller is to minimize an economic objective by determining the energy flows within the system. HMPC enables a long-term scheduling solution to anticipate ahead of the seasonal energy mismatches occurring in PtX systems. This paper presents a novel approach to couple the separate control layers in the hierarchy by heuristic assignment to fully employ the PtX fundamentals in the controller design. Simulation results based on historical data of the Dutch energy sector show the suitability of HMPC and its superiority over a rule-based control approach. The proposed controller may, however, also be used for any configuration of multi-timescale mixed-energy systems dealing with temporal energy mismatches.**

Index Terms—**Multi-Energy Systems, Power to X, Model Predictive Control, Multi-Time Scale, Economic Dispatch**

I. Introduction

The penetration of renewable energy sources (RES) in the grid is quickly proceeding due to the global effort to reduce CO_2 emissions. The power generated by RES is heavily subject to the intermittency of the source, e.g., availability of solar irradiance. Therefore, there are periods with excess power availability in the grid, where the excess is curtailed or exported. On the other hand, there are periods of lack of production, then power must be imported, or more expensive and/or polluting units must be deployed to produce electricity. This intermittent behavior may cause a strain on the future power grids when more RES are deployed, and bi-directional flows between residential power producers and the grid will be more common [1].

Power-to-X (PtX) strategies aim to utilize the excess power from RES by converting power to another energy carrier, e.g., heat. By allowing the transition of power to another energy carrier, the system is transformed into a so-called multi-energy system. This formulation allows for optimal scheduling of energy flows in the system while taking into account the characteristics of each energy carrier, e.g., storage characteristics, time-varying costs, or production emissions. Therefore, the system takes into account the multiple energy carriers' system characteristics and loads in an integrated way. This paper considers a neighborhood-sized PtX system that is able to locally produce and meet the demands of multiple energy carriers. The underlying power network of such a system is generally a grid-connected microgrid. Therefore, control methods for microgrids are also suitable for PtX systems.

The main challenge of PtX control, as opposed to the control of microgrids, is finding a way to deal with the temporal mismatch between energy production and consumption. The most apparent temporal mismatch happens between power and heat, where peaks of power generation are expected in the summer, and in the winter, heat demands would spike. An Aquifer Thermal Energy Storage (ATES) was included in this paper for storing thermal energy for multiple months. Moreover, similarly to microgrid control, an intelligent energy management system (EMS) is essential in PtX systems to determine the optimal energy flows while attaining the desired goal, e.g., an economic one. Some decisions the EMS has to make are:

- how much of a particular energy carrier should be generated or produced to meet that energy carriers load at minimal economic cost (energy dispatch);
- when each generation unit should be started and stopped (unit commitment);
- whether and how much of a certain energy carrier is exchanged with an external party, e.g., utility grid;
- how much of a particular energy carrier is stored or taken from the corresponding storages.

In recent literature, Model Predictive Control (MPC) is widely applied as an EMS of microgrids. Generally, the EMS determines set-points for low-level control units to track. Several works are using the MPC framework to deal with multi-timescale systems. The multi-layered approach, i.e., Hierarchical MPC (HMPC) was used in [2] and [3] as EMS of microgrids. Moreover, a single-layer approach was given in [4] for microgrids and [5] used a move-blocking scheme for heating networks dealing with multiple time scales.

The main contribution of this work is the application of MPC on PtX systems. Furthermore, the development of an HMPC controller for the optimized energy management for PtX systems dealing with temporal energy mismatches is shown. For the HMPC scheme a novel heuristic controller coupling based on PtX principles is introduced. Meaning, the computed reference value from the long-term scheduling upper-layer controller is proportionally divided by the sum of the total forecasted solar power. By doing so, the reference is only changed when there is an excess of power available.

The outline of this paper is as follows. Section II describes the PtX system considered in this paper, along with modeling decisions. In Section III an HMPC approach is presented, and in Section IV case study results are shown to assess the

O. Kaya (Oguzhan_Kaya96@hotmail.com) and T. Keviczky (T.Keviczky@tudelft.nl) are with the Delft Center for Systems and Control, Delft University of Technology in Delft, The Netherlands. E. van der Roest (Els.van.der.Roest@kwrwater.nl) and D. Vries (Dirk.Vries@kwrwater.nl) are with KWR Watercycle Research Centre in Nieuwegein, The Netherlands.

controller and compare with a rule-based controller. The paper is concluded in Section V.

II. Power-to-X System

We consider a PtX system consisting of a microgrid, district heating network, and hydrogen and water services. The power is generated by a local solar farm and the microgrid operates in grid-connected mode. The energy carriers may be stored in their corresponding storage unit, whereas thermal energy can be stored for multiple months in an ATES. The goal is to design an EMS to minimize the operational expenses while balancing the local production and consumption of each energy carrier. Fig. 1 illustrates an energy flow diagram of the system.

Remark. Electrical demands are not taken into account for the global energy balance, due to regulations in the Netherlands.

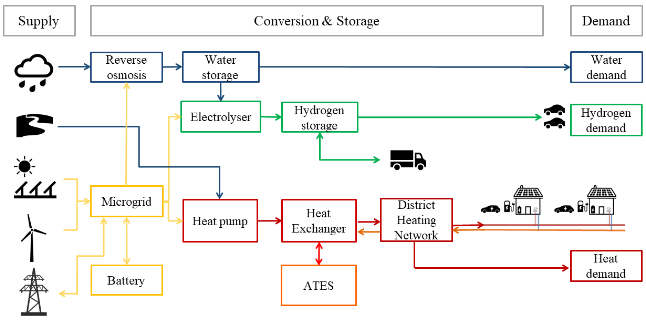

Fig. 1. Energy flow diagram of the PtX system. The energy carriers in the system are electricity (yellow), thermal energy (red and orange), hydrogen (green), and water (blue), and are indicated by arrows.

Remark. The notation in this work is as follows. Scalars are written as lowercase letters, e.g., a, matrices as written in bold uppercase letters, e.g., $\boldsymbol{A}$. Moreover, discrete-time instants are expressed with k and discrete-time sampling intervals are written as τ. Storage and conversion efficiencies are denoted as η.

A. Microgrid

1) Battery Energy Storage System Model: The dynamics of the Battery Energy Storage System (BESS) were adopted from [6] and are given by the following Mixed-Logical Dynamical (MLD) system:

$$x_{\mathrm{b}}(k+1) = x_{\mathrm{b}}(k) - (\eta_{\mathrm{dch}} - \eta_{\mathrm{ch}})z_{\mathrm{b}}(k)\tau + \eta_{\mathrm{dch}}P_{\mathrm{b}}(k)\tau, \quad (1)$$

$$\text{s.t.} \quad \boldsymbol{E}_{\mathbf{b1}}\delta_{\mathrm{b}}(k) + \boldsymbol{E}_{\mathbf{b2}}z_{\mathrm{b}}(k)\tau \leq \boldsymbol{E}_{\mathbf{b3}}P_{\mathrm{b}}(k)\tau + \boldsymbol{E}_{\mathbf{b4}}, \quad (2)$$

where x_{b} is the BESS state of charge, $z_{\mathrm{b}} := \delta_{\mathrm{b}}P_{\mathrm{b}}$ the MLD auxiliary variable, δ_{b} the boolean variable indicating the BESS mode, i.e. charging or discharging and P_{b} the power exchanged with the BESS. Details on MLD system matrices, denoted by $\boldsymbol{E}$, can be found in [6].

2) External Grid Interaction: The microgrid under consideration will exclusively operate in grid-connected mode. Thus it is always possible to exchange energy with the external utility grid. We assume that different prices are governed for import and export and that these prices are time-varying. Furthermore, it is assumed that at each time instant the import price is larger than the exporting price. The variable C_{grid} represents the cost or revenue due to interaction with the utility grid and is given by:

$$C_{\mathrm{grid}}(k) = \max(c_{\mathrm{e,imp}}(k)P_{\mathrm{grid}}(k)\tau, c_{\mathrm{e,exp}}(k)P_{\mathrm{grid}}(k)\tau), \quad (3)$$

where P_{g} is the power exchanged with the grid, $c_{\mathrm{e,imp}}$ and $c_{\mathrm{e,exp}}$ are the import and export price of electricity and $c_{\mathrm{e,imp}} \geq c_{\mathrm{e,exp}}$.

3) Energy Balance: The energy demands in the system must be met at each time instant. The following inequality captures the energy balance:

$$E_{\mathrm{pv}}(k) + \big(P_{\mathrm{grid}}(k) - P_{\mathrm{b}}(k) - P_{\mathrm{hp}}(k) \quad (4)$$
$$P_{\mathrm{el}}(k) - P_{\mathrm{ro}}(k)\big)\tau \geq 0, \quad (5)$$

where E_{pv} is the generated energy from PV generation, P_{hp} is the power input to the heat pump, P_{el} power input of the electrolyzer and P_{ro} the power consumption of the reverse osmosis system.

B. Heat System

1) Aquifer Thermal Energy Storage Modeling: ATES is a cost-efficient seasonal storage system that can be used to store large quantities of thermal energy. In its purest form, two wells are formed underground as porous formations, also known as aquifers. The system consists of a hot and cold well to store hot and cold water depending on the season. The heat from the stored water in the hot well can be extracted by pumping the water from the hot well to the cold well through a heat exchanger. Similarly, heat can be stored by pumping water from the cold well to the hot well while providing the water with thermal energy from a heat pump. The ATES dynamical system is given by:

$$S_{\mathrm{h}}(k+1) = \eta_{\mathrm{h}}(k)S_{\mathrm{h}}(k) - \alpha_{\mathrm{h}}u_a(k)\tau, \quad (6)$$
$$S_{\mathrm{c}}(k+1) = \eta_{\mathrm{c}}(k)S_{\mathrm{c}}(k) + \alpha_{\mathrm{c}}u_a(k)\tau, \quad (7)$$

where the state S denotes the thermal energy content and u_{a} is the control input corresponding to the pump flow rate of the system. The subscripts 'h' and 'c' denote the hot and cold well, respectively. The wells are characterized by their storage efficiencies η and thermal power coefficients α.

2) Heat Pump Modeling: A heat pump is a device that transfers heat from a low-temperature zone to a higher-temperature zone using mechanical work. Generally, a heat pump draws heat from the air, ground or water and uses a vapor compression refrigeration cycle. We assume the heat is drawn from water originating from a nearby river. The output thermal energy of the heat pump delivered at each time step can be calculated by:

$$Q_{\mathrm{hp}}(k) = \mathrm{COP}(k) \cdot P_{\mathrm{hp}}(k)\tau, \quad (8)$$

where Q_{hp} is the output thermal energy of the heat pump and P_{hp} is the input power of the heat pump and COP is the coefficient of performance.

3) District Heating Network Model: At each time instant, the thermal energy in the district heating system must be equal or larger than the thermal demand of its users. The following constraint captures the thermal energy balance:

$$Q_{\text{hp}}(k) - Q_{\text{ATES}}(k) - Q_{\text{d}}(k) \geq 0, \tag{9}$$

where Q_{d} is the uncertain variable denoting the thermal energy demand of the system and Q_{ATES} is the thermal energy exchange with ATES, i.e., $Q_{\text{ATES}} = (\alpha_{\text{h}} + \alpha_{\text{c}})u_{\text{a}}\tau$. We assume that temperature in the wells and the ambient temperature are constant, which means the system is no longer time-varying. It is also assumed that we can continue extracting water from the wells when they are fully depleted. This means we are extracting water with ambient temperature. The total power coefficients depend on the flow direction of the pump and the current thermal energy contents of the well. The ATES dynamics can be rewritten into a piecewise-affine (PWA) function. Subsequently, by using HYSDEL [7] in Matlab, (9) and the PWA ATES dynamics can be transformed into an MLD system: Now let us define $\boldsymbol{x}_{\text{a}}^T = \begin{bmatrix} S_{\text{h}} & S_{\text{c}} \end{bmatrix}^T$ and consider the following discrict heating network system:

$$\boldsymbol{x}_{\text{a}}(k+1) = \boldsymbol{A}_{\text{a}}(k)\boldsymbol{x}_{\text{a}}(k) + \boldsymbol{B}_{\text{a}}(k)u_{\text{a}}(k)\tau, \tag{10}$$

$$Q_{\text{hp}}(k) = \boldsymbol{D}_{\text{a}}\boldsymbol{z}_{\text{a}}(k) + Q_{\text{d}}(k), \tag{11}$$

$$\boldsymbol{E}_{\text{a1}}\boldsymbol{x}_{\text{a}}(k) + \boldsymbol{E}_{\text{a2}}u_{\text{a}}(k)\tau + \boldsymbol{E}_{\text{a3}}\boldsymbol{z}_{\text{a}}(k)\tau + \boldsymbol{E}_{\text{a4}}\boldsymbol{\delta}_{\text{a}}(k) \leq \boldsymbol{E}_{\text{aff}}, \tag{12}$$

where $\boldsymbol{z}_{\text{a}}^T$ and $\boldsymbol{\delta}_{\text{a}}^T$ denote the vector of auxiliary and binary variables, respectively. The full MLD system derivation and MLD system matrices, denoted by $\boldsymbol{E}$, can be found in [8].

C. Hydrogen and Water Systems

1) Modeling Hydrogen Trades: Similar to the electricity utility interaction, hydrogen may also be imported or exported. The hydrogen prices are assumed to be constant, and again the importing price is larger than the exporting price.

$$C_{\text{hy}}(k) = \max(c_{\text{hy,imp}}H_{\text{trade}}(k), c_{\text{hy,exp}}H_{\text{trade}}(k)), \tag{13}$$

where C_{hy} is the cost or revenue of trading hydrogen, $c_{\text{hy,imp}}$ and $c_{\text{hy,exp}}$ the import and export price of hydrogen, respectively and H_{trade} is the amount of hydrogen traded.

2) Hydrogen Production and Storage Modeling: A water electrolysis system is responsible for providing the hydrogen needed for mobility purposes in the neighborhood. The produced hydrogen is assumed to be stored directly in a connected reservoir. We assume that the energy consumption of the electrolysis system, P_{el} is a linear function of the produced hydrogen. Now the hydrogen storage's dynamics are given by:

$$x_{\text{el}}(k+1) = x_{\text{el}}(k) + H_{\text{el}}(k) + H_{\text{trade}}(k) - H_{\text{d}}(k), \tag{14}$$

where x_{el} denotes the state of the electrolyzer's hydrogen buffer, H_{el} the produced hydrogen and H_{d} the uncertain hydrogen demand.

3) Water Production and Storage Modeling: Demiwater, also known as demineralized water is used in the system for the production of hydrogen and in residential use, e.g., dishwashers and washing machines. A high-pressure pump, a membrane module, and water storage tank form the reverse osmosis system for the production of demiwater. Generally, water is pressurized and fed into the system where it is separated into a low-salinity product (permeate), and a high-salinity brine (retentate). The demiwater can now either be used to meet the water demand or stored in a water tank. Based on the latter introduction, the dynamics of the volume in the storage tank, x_{dw} is given by:

$$x_{\text{dw}}(k+1) = x_{\text{dw}}(k) + F_{\text{ro}}(k)\tau - \eta_{\text{hy,dw}} \cdot H_{\text{el}}(k)\tau - F_{\text{d}}(k), \tag{15}$$

where x_{dw} is the storage volume and F_{ro} the produced demiwater and F_{d} the demiwater demand.

III. Hierarchical Model Predictive Control Framework

The HMPC framework generally aims to partition the control of multiple timescales within a system and assign them to a separate layer in the control hierarchy. In this work, the proposed HMPC scheme is depicted in Fig. 2 and consists of two layers.

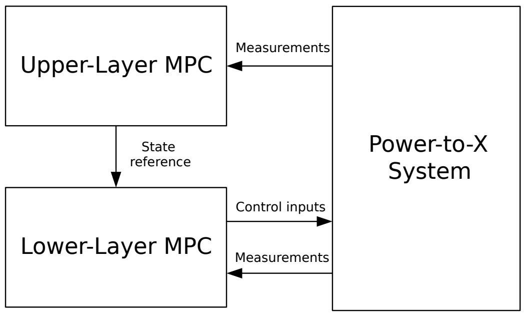

Fig. 2. HMPC control scheme consisting of the UL-MPC and LL-MPC controllers.

A. Upper-Layer MPC Design

The Upper-Layer MPC (UL-MPC) controller is designed for long-term decision making of ATES storage planning and providing its decision as reference for the Lower-Layer MPC (LL-MPC). The temporal energy discrepancies are visible over multiple months, therefore, the sampling time τ^{u} is chosen to be a month. The upper-layer prediction horizon is $N^{\text{u}} = 12$ months, i.e. a year. The UL-MPC dynamical model only consists of the heat system (10), (11) and (12). At each time instant k^{u} the following linear cost function is minimized:

$$J^{\text{u}} = \sum_{i=0}^{N^{\text{u}}-1} \left(C_{\text{grid}}(k^{\text{u}}+i|k^{\text{u}}) + C_{\text{hy}}(k^{\text{u}}+i|k^{\text{u}}) \right), \tag{16}$$

subject to system dynamics (10), (11) and (12), state and input constraints:

$$\underline{\boldsymbol{x}}_{\text{a}} \leq \boldsymbol{x}_{\text{a}}(k^{\text{u}}+i|k^{\text{u}}) \leq \overline{\boldsymbol{x}}_{\text{a}} \quad \forall i=0,\dots,N^{\text{u}}-1, \tag{17}$$

$$\underline{u}_{\text{a}} \leq u_{\text{a}}(k^{\text{u}}+i|k^{\text{u}}) \leq \overline{u}_{\text{a}} \quad \forall i=0,\dots,N^{\text{u}}-1, \tag{18}$$

energy balance:

$$E_{\text{pv}}(k^{\text{u}}+i|k^{\text{u}}) + P_{\text{grid}}(k^{\text{u}}+i|k^{\text{u}})\tau^{\text{u}} - P_{\text{hp}}(k^{\text{u}}+i|k^{\text{u}})\tau^{\text{u}} - P_{\text{el}}(k^{\text{u}}+i|k^{\text{u}})\tau^{\text{u}} - P_{\text{ro}}(k^{\text{u}}+i|k^{\text{u}})\tau^{\text{u}} \geq 0 \quad \forall i=0,\dots,N^{\text{u}}-1, \tag{19}$$

and mass balances:

$$H_{\text{el}}(k^{\text{u}}+i|k^{\text{u}})\tau^{\text{u}} + H_{\text{trade}}(k^{\text{u}}+i|k^{\text{u}})\tau^{\text{u}} - H^{\text{u}}_{\text{d}}(k^{\text{u}}+i|k^{\text{u}}) \geq 0 \tag{20}$$

$$F_{\text{ro}}(k^{\text{u}}+i|k^{\text{u}})\tau^{\text{u}} - \eta_{\text{hy,dw}} \cdot H_{\text{el}}(k^{\text{u}}+i|k^{\text{u}}) - F_{\text{d}}(k^{\text{u}}+i|k^{\text{u}}) \geq 0 \tag{21}$$

$$\forall i=0,\dots,N^{\text{u}}-1$$

B. Lower-Layer MPC Design

The LL-MPC is the actual EMS of the PtX system providing hourly set-points to the system. The lower-layer sampling time is $\tau^{\text{l}} = 1$ hour and the prediction horizon is chosen to be $N^{\text{l}} = 24$ hours. At each time instant k^{l} the following cost function is minimized:

$$J^{\text{l}} = \sum_{i=0}^{N^{\text{l}}-1} \left(C_{\text{grid}}(k^{\text{l}}+i|k^{\text{l}}) + C_{\text{hy}}(k^{\text{l}}+i|k^{\text{l}})\right) + \sum_{i=0}^{N^{\text{l}}} \left(|S_{\text{h}}(k^{\text{l}}+1+i|k^{\text{l}}) - S_{\text{ref}}(k^{\text{l}}+i|k^{\text{l}})|\right), \tag{22}$$

subject to storage dynamics (1), (2), (10)-(12), (14) and (15), state and input constraints, and energy balance constraint:

$$E_{\text{pv}}(k^{\text{l}}+i|k^{\text{l}}) + P_{\text{grid}}(k^{\text{l}}+i|k^{\text{l}})\tau^{\text{l}} - P_{\text{b}}(k^{\text{l}}+i|k^{\text{l}})\tau^{\text{l}} - P_{\text{hp}}(k^{\text{l}}+i|k^{\text{l}})\tau^{\text{l}} - P_{\text{el}}(k^{\text{l}}+i|k^{\text{l}})\tau^{\text{l}} - P_{\text{ro}}(k^{\text{l}}+i|k^{\text{l}})\tau^{\text{l}} \geq 0 \tag{23}$$

C. Controller Coupling

The UL-MPC generates monthly setpoints for the LL-MPC by updating the model output, i.e. $S^*_{\text{h}}(k^u+1|k^u)$ by applying the first input of the calculated optimal control sequence in (10). Two ways to utilize the setpoint are investigated. The first method is a linear interpolation [9], whereas the second method consists of heuristic weight assignments. The heuristic assignment is done by proportionally dividing the setpoint in a month by the solar power availability when storing heat, and heating demand when using heat from the storage. In Fig. 3 the working principles of both are methods are shown.

1) Linear Interpolation: The calculation of the reference sequence by the linear interpolation methods is given by:

$$S_{\text{ref}}(k^{\text{l}}+i|k^{\text{l}}) = S_{\text{h}}(k^{\text{l}}|k^{\text{l}}) + \frac{i+1}{720 \cdot k^{\text{u}} - k^{\text{l}}} \cdot \left(S^*_{\text{h}}(k^u+1|k^u) - S_{\text{h}}(k^{\text{l}}|k^{\text{l}})\right) \quad \forall i=0,\dots,N^{\text{l}}-1 \tag{24}$$

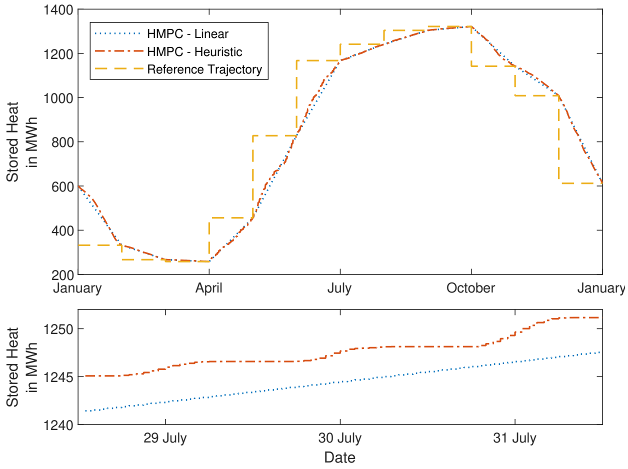

Fig. 3. ATES thermal energy content for a year (upper figure) and for a few days in the summer (lower figure).

2) Heuristic Assignment: The heuristic assignment for months when heat is stored is given by:

$$S_{\text{ref}}(k^{\text{l}}+i|k^{\text{l}}) = S_{\text{h}}(k^{\text{l}}|k^{\text{l}}) + \frac{\sum_{j=0}^{i+1} E_{\text{pv}}(k^{\text{l}}+j|k^{\text{l}})}{E_{\text{pv}}(k^u)} \cdot \left(S^*_{\text{h}}(k^{\text{u}}+1|k^{\text{u}}) - S_{\text{h}}(k^{\text{l}}|k^{\text{l}})\right) \quad \forall i=0,\dots,N^{\text{l}}-1 \tag{25}$$

This assignment makes sure that heat is only produced when there is solar power available. Thus fully employing the PtX principles of utilizing excess power. Furthermore, the assignment for months when heat is used from the storage is given by:

$$S_{\text{ref}}(k^{\text{l}}+i|k^{\text{l}}) = S_{\text{h}}(k^{\text{l}}|k^{\text{l}}) + \frac{\sum_{j=0}^{i+1} Q_{\text{d}}(k^{\text{l}}+j|k^{\text{l}})}{Q_{\text{d}}(k^u)} \cdot \left(S_{\text{h}}(k^{\text{l}}|k^{\text{l}}) - S^*_{\text{h}}(k^{\text{u}}+1|k^{\text{u}})\right) \quad \forall i=0,\dots,N^{\text{l}}-1 \tag{26}$$

D. Dealing with Uncertainties

To operate an MPC controller as EMS in real-life applications one must deal with the uncertainties acting on the system. In this work we have been introduced to the following uncertain variables, E_{pv}, Q_{d}, H_{d} and F_{d}. Since the LL-MPC has a prediction horizon of a day, there must be predictions available for the uncertain variables. We have chosen to use the 'naive' persistence model, in which we assume that the future uncertainties are the same as the measurements the day before. In the deterministic framework, these 'forecasts' are assumed to be correct and directly used in the UL-MPC and LL-MPC control problems, also known as *certainty-equivalent MPC* (CEMPC). Moreover, *scenario-based MPC* (SBMPC) was applied as described in [10]. Due to the imperfect knowledge of the future trajectories of the uncertainties, constraint violations may occur. Where the CEMPC controller cannot guarantee any constraint satisfaction, the SBMPC approach uses finite scenario realizations of the disturbances to guarantee the satisfaction of constraints with a predefined violation risk.

We assume that the external grid reacts fast enough to deal with electrical energy imbalances. Furthermore, it is also assumed that the heat pump's power setpoint can be adjusted fast enough to deal with heat balance mismatch. At last, conservative lower bounds for hydrogen and water storage units are applied to intercept imbalances.

IV. Simulation Results

The HMPC schemes presented in Section III will be assessed in a case study based on historical data of the Dutch energy sector. A rule-based control law was developed for benchmark purposes. Moreover, the HMPC optimal control problem is a Mixed-Integer Linear one. The optimization was formulated with the YALMIP toolbox [11] and solved with GUROBI solver in Matlab.

Fig. 4 shows the storage utilization for a few summer days for the CEMPC controllers. Both HMPC schemes decide to fill the BESS and water storage during the day when there is an excess of solar energy. These supplies are then used during the night. Moreover, in the bottom graph of Fig. 3 the difference during the day of both HMPC schemes was highlighted, i.e. constant heat production vs. producing heat when there is solar power available.

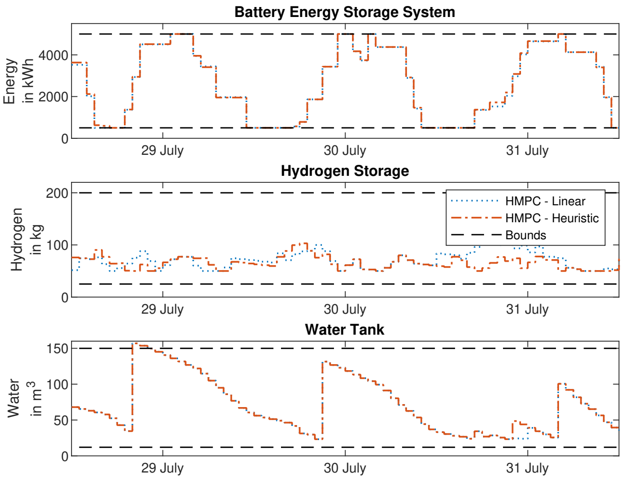

Fig. 4. Simulation results of storage utilization for a few summer days.

The control strategies will be compared based on the following performance indices. The yearly revenue, which is directly incorporated in the MPC optimization formulation, the carbon-dioxide emission savings in a year and the amount of heat left in the ATES hot well at the end of the simulation. These results for the CEMPC controllers are presented in Table. I. Since the operational expenses were the only performance index to be incorporated in the controller design, the best value was highlighted in the table.

The SBMPC controllers yielded slightly less yearly revenue, with the benefit of less constraint violations. What is significant to note is that the grid capacity for importing was never exceeded. Hence no adverse penalties on grid capacity violation were imposed on the controllers. Therefore, it is important to emphasize that any other PtX configuration may lead to better performing SBMPC controllers.

TABLE I

Performance Indices of Assessed Control Schemes

Control Strategy	**Rule-Based Control**	**HMPC Linear**	**HMPC Heuristic**
Yearly Revenue in €	$9.45 \cdot 10^4$	$2.19 \cdot 10^5$	$\mathbf{2.22 \cdot 10^5}$
Emission Savings in tonnes	$7.00 \cdot 10^2$	$3.29 \cdot 10^2$	$3.73 \cdot 10^2$
Heat Storage in MWh	0.00	0.626	0.626

V. Conclusions

This paper presented an HMPC approach for optimizing the energy flows within a PtX system consisting of multiple timescales. We have presented two variants of the HMPC controller, a linear interpolation and heuristic controller coupling. Including heuristics in the HMPC controller coupling yielded better performance. With improved forecasts, this controller still has as much as 55% to improve in yearly revenue (CEMPC). Simulations show that the proposed approach achieves better performance than a rule-based approach.

Future work includes the addition of electrical loads, an HMPC approach with event-driven updates, improving forecasts, and performing a simulation based on the ATES simulation environment MODFLOW.

References

[1] N. Hatziargyriou, H. Asano, R. Iravani, C. Marnay, "Microgrids," in IEEE Power and Energy Magazine, vol. 5, no. 4, pp. 78-94, 2007

[2] X. Xu, H. Jia, D. Wang, D. C. Yu, H.-D. Chiang, "Hierarchical energy management system for multi-source multi-product microgrids," Renewable Energy, vol. 78, pp. 621–630, 2015.

[3] S. Raimondi Cominesi, M. Farina, L. Giulioni, B. Picasso, R. Scattolini, "A two-layer stochastic model predictive control scheme for microgrids," in IEEE Transactions on Control Systems Technology, vol. 26, no. 1, pp. 1-13, 2018.

[4] T. Pippia, J. Sijs, B. De Schutter, "A parametrized model predictive control approach for microgrids," 2018 IEEE Conference on Decision and Control, Miami Beach, FL, 2018, pp. 3171-3176.

[5] V. Rostampour, T. Keviczky, "Probabilistic energy management for building climate comfort in smart thermal grids with seasonal storage systems," in IEEE Transactions on Smart Grid, vol. 10, no. 4, pp. 3687-3697, 2019.

[6] A. Parisio, E. Rikos, "Stochastic model predictive control for economic/environmental operation management of microgrids: an experimental case study," Journal of Process Control 43, 2016, pp. 24-37.

[7] F. D. Torrisi, A. Bemporad, "HYSDEL-a tool for generating computational hybrid models for analysis and synthesis problems," in IEEE Transactions on Control Systems Technology, vol. 12, no. 2, pp. 235-249, 2004.

[8] O. Kaya, "Hierarchical MPC for Energy Management of Multi-Energy Systems", Master's thesis, Delft University of Technology, Delft, 2020.

[9] M. Joševski, D. Abel, "Multi-time scale model predictive control framework for energy management of hybrid electric vehicles," 53rd IEEE Conference on Decision and Control, Los Angeles, CA, pp. 2523-2528, 2014.

[10] A. Parisio, D. Varagnolo, M. Molinari, G. Pattarello, L. Fabietti, K. H. Johansson "Implementation of a scenario-based mpc for hvac systems: an experimental case study." IFAC Proceedings Volumes, vol. 47.3, pp. 599-605, 2014.

[11] J. Lofberg, "YALMIP: a toolbox for modeling and optimization in MATLAB," 2004 IEEE International Conference on Robotics and Automation, New Orleans, LA, pp. 284-289, 2004.